

Single or multi-flavor Kondo effect in graphene

Zhen-Gang Zhu¹, Kai-He Ding², Jamal Berakdar¹

¹*Institut für Physik, Martin-Luther-Universität Halle-Wittenberg,
Nanotechnikum-Weinberg, Heinrich-Damerow-St. 4, 06120 Halle, Germany;*

²*Department of Physics and Electronic Science,
Changsha University of Science and Technology, Changsha 410076, China*

Abstract

Based on the tight-binding formalism, we investigate the Anderson and the Kondo model for an adatom magnetic impurity above graphene. Different impurity positions are analyzed. Employing a partial wave representation we study the nature of the coupling between the impurity and the conducting electrons. The components from the two Dirac points are mixed while interacting with the impurity. Two configurations are considered explicitly: the adatom is above one atom (ADA), the other case is the adatom above the center the honeycomb (ADC). For ADA the impurity is coupled with one flavor for both A and B sublattice and both Dirac points. For ADC the impurity couples with multi-flavor states for a spinor state of the impurity. We show, explicitly for a 3d magnetic atom, d_{z^2} , (d_{xz}, d_{yz}) , and $(d_{x^2-y^2}, d_{xy})$ couple respectively with the Γ_1 , $\Gamma_5(E_1)$, and $\Gamma_6(E_2)$ representations (reps) of C_{6v} group in ADC case. The bases for these reps of graphene are also derived explicitly. For ADA we calculate the Kondo temperature.

PACS numbers: 75.20.Hr, 72.15.Qm, 71.55.-i, 81.05.ue

INTRODUCTION

In Graphene, a monolayer of carbon atoms recently fabricated successfully [1], the valence and the conduction bands touch at two inequivalent Dirac points K_- and K_+ at the corners of the first Brillouin zone (FBZ). Near K_- and K_+ the low energy dispersion is linear, indicating a massless Dirac fermions behavior. This particular band structure is at the heart of a number of unusual electronic properties [2]. Graphene is also an interesting candidate for transport-applications, in particular for spintronics: It exhibits a remarkably high mobility and the carrier density is controllable by a gate voltage; the mean free path can be as large as $1\ \mu m$. Graphene is however not immune to disorder that influences its electronic properties [2]. Extrinsic disorder is realized in a variety of ways: adatoms, vacancies, charges on top of graphene or in the substrates, and extended defects such as cracks and edges. When localized magnetic impurities are added [3] the Kondo effect, i.e. the dynamic screening of the localized moment, has to be addressed at temperatures T below the Kondo temperature T_K . In this context, previous studies addressed the influence of magnetic impurities using the Hartree-Fock approximation [4, 5] which is valid at $T > T_K$ (see also [6]). In Ref. [7] the anisotropic *single* channel Kondo model is investigated briefly and in Ref. [8] the *infinite- U* Anderson model for an impurity embedded in a graphene sheet has been employed and concluded a Fermi liquid behaviour. Recently, it has been claimed that a two-channel Kondo in graphene is present due to the *valley degeneracy* of the Dirac electrons [9], which leads to an over-screening and thus to a non-Fermi-liquid-like ground state. Very recently Refs. [10, 11] reported on scanning tunneling spectroscopy studies to investigate the Kondo effect in graphene. *All* of these studies consider a particular configuration of the impurity. In this work, we show that the position of the impurity on or in graphene plays a subtle role and affects essentially the underlying physics. In addition to the role of the vanishing density of state (DOS) at the Dirac points and the linear spectrum in their vicinity, a further important issue is to clarify whether a single or a multi-channel Kondo problem is realized. This is insofar important as the ground states for these two cases are essentially different: As established [12], when the channel number N_{cha} is equal to $2S_{\text{im}}$ (S_{im} is the spin of the impurity), the impurity spin is then compensated by the host electrons completely, resulting in a singlet Fermi liquid ground state. When $N_{\text{cha}} > 2S_{\text{im}}$ we enter the over-compensated regime where an opposite spin to the original spin appears and acts as

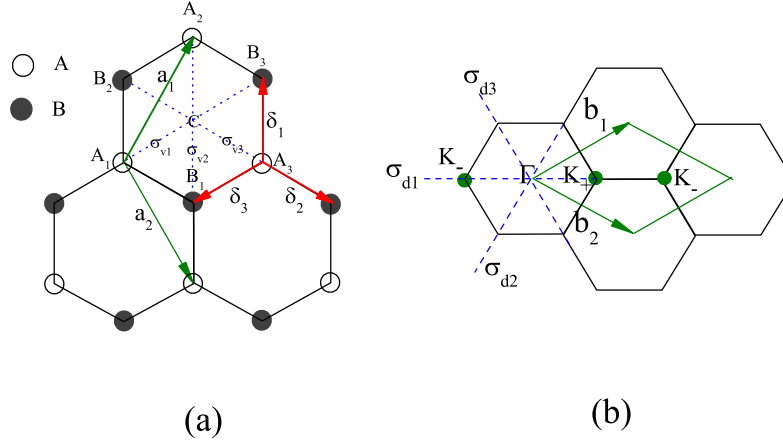


FIG. 1: (color online). (a) shows graphene primitive vectors and the symmetry operations defining the group of the crystal, $\sigma_{vi}, i = 1, 2, 3$ are reflection planes showing up in C_{6v} little group at Γ point. (b) shows FBZ with the symmetry operations (see text for explanations).

a remainder spin; an effective antiferromagnetic coupling between this remainder effective impurity spin and the conducting spins results in a non-Fermi liquid ground state [13–15]. Thus, it is crucial to clarify when graphene with an impurity with a spin one-half is a single or a two channels Kondo system. Recently, scanning tunneling conductance spectra are investigated with respect to the position of the scanning tip in Refs. [16, 17] (see also Ref. [18]).

As a first essential step we identify the physical origin of the multi channels for the Kondo effect by analyzing the tight-binding Anderson model [19, 20]. A partial wave method is then employed to reduce the redundant flavors and to identify the coupling flavors. The role of the Dirac points is exposed. An adatom above one carbon atom (ADA) or an adatom above the center of the honeycomb (ADC) configurations are considered.

THEORETICAL FORMULATION

We start from the Anderson Hamiltonian

$$H = H_g + H_f + H_{\text{hyb}}. \quad (1)$$

H_g (H_f) describes graphene, (impurity) and H_{hyb} stands for the impurity-graphene hybridization. The graphene primitive vectors are $\mathbf{a}_1 = a(\frac{1}{2}, \frac{\sqrt{3}}{2})$, $\mathbf{a}_2 = a(\frac{1}{2}, -\frac{\sqrt{3}}{2})$, where $a = \sqrt{3}a_{\text{cc}}$, a_{cc} is the distance of the nearest carbon atoms. The B sublattice is related to A sublattice by $\boldsymbol{\delta}_1 = (\mathbf{a}_1 - \mathbf{a}_2)/3$, $\boldsymbol{\delta}_2 = \mathbf{a}_1/3 + 2\mathbf{a}_2/3$, and $\boldsymbol{\delta}_3 = -\boldsymbol{\delta}_1 - \boldsymbol{\delta}_2 = -2\mathbf{a}_1/3 - \mathbf{a}_2/3$ (cf. Fig. 1(a)). The two inequivalent Dirac points in FBZ are $\mathbf{K}_{\pm} = \pm \frac{2\pi}{a}(2/3, 0)$. The second quantization tight-binding-Hamiltonian [2, 4, 21–23] reads $H_g = \sum_{\langle ij \rangle \sigma} (t a_{i\sigma}^\dagger b_{j\sigma} + t^* b_{j\sigma}^\dagger a_{i\sigma})$ where the sum runs over the nearest-neighbor pairs $\langle ij \rangle$, σ is a spin index, and $a_{i\sigma}$ ($b_{i\sigma}$) are annihilation operators for states on the A (B) sublattice. The Hamiltonian in momentum space is $H_g = \sum_{\bar{\mathbf{k}}\sigma} [\xi(\bar{\mathbf{k}}) a_{\bar{\mathbf{k}}\sigma}^\dagger b_{\bar{\mathbf{k}}\sigma} + \xi^*(\bar{\mathbf{k}}) b_{\bar{\mathbf{k}}\sigma}^\dagger a_{\bar{\mathbf{k}}\sigma}]$, where $\xi(\bar{\mathbf{k}}) = -t\Phi(\bar{\mathbf{k}})$, $\Phi(\bar{\mathbf{k}}) = \sum_{\boldsymbol{\delta}_i} e^{i\bar{\mathbf{k}} \cdot \boldsymbol{\delta}_i}$, and $\bar{\mathbf{k}}$ are wave vectors in FBZ. The hybridization Hamiltonian in tight-binding formalism is $H_{\text{hyb}} = \sum_{\bar{\mathbf{k}}\sigma} [(V_{\bar{\mathbf{k}}}^{Af} a_{\bar{\mathbf{k}}\sigma}^\dagger f_\sigma + V_{\bar{\mathbf{k}}}^{Bf} b_{\bar{\mathbf{k}}\sigma}^\dagger f_\sigma) + h.c.]$, where $V_{\bar{\mathbf{k}}}^{\alpha f} = \frac{1}{\sqrt{N}} \sum_{\mathbf{R}_i \neq \mathbf{R}_{\text{im}}} e^{-i\bar{\mathbf{k}} \cdot (\mathbf{R}_i + \boldsymbol{\tau}_\alpha)} V^{\alpha f}(\mathbf{R}_i + \boldsymbol{\tau}_\alpha - \mathbf{R}_{\text{im}})$, $\alpha = \text{A or B}$, $\boldsymbol{\tau}_\alpha$ stands for the relative location for α atom in the unit cell, $V^{\alpha f}(\mathbf{R}_i + \boldsymbol{\tau}_\alpha - \mathbf{R}_{\text{im}}) = \int d\mathbf{r} [\phi^\alpha(\mathbf{r} - \mathbf{R}_i - \boldsymbol{\tau}_\alpha)]^* h(\mathbf{r}) \phi_L(\mathbf{r} - \mathbf{R}_{\text{im}})$, and ϕ^α is the atomic function for the atoms in α sublattice (only π orbitals are included), ϕ_L is the localized impurity wave function, h is the single particle Hamiltonian, and N is the number of unit cells.

$V^{\alpha f}(\mathbf{R}_i + \boldsymbol{\tau}_\alpha - \mathbf{R}_{\text{im}})$ is a Slater-type bond in LCAO formalism [24] which describes the strength of hybridization between two atomic orbitals located at the impurity and its neighbors. Here only p_π electrons are relevant. They form the π and π^* which touch at the Dirac points \mathbf{K}_{\pm} . An s-wave impurity substituting one carbon atom in the graphene plane is decoupled from π and π^* bands; for d- and f-wave impurity in this substitution case is possible. Our focus is however on the case where the impurity is above the graphene plane. The relative positions of the impurity determine the hybridization strength, i.e. $V^{\alpha f}$ and the phase is included in the exponential in $V_{\bar{\mathbf{k}}}^{\alpha f}$.

To obtain an effective low-energy Hamiltonian we expand the wave vector $\bar{\mathbf{k}} = \mathbf{K}_{\pm} + \mathbf{k}$ around \mathbf{K}_{\pm} . Thus, $\Phi(\bar{\mathbf{k}}) \approx (-v_F/t)(\pm k_x - i k_y)$, or $\Phi(\bar{\mathbf{k}})|_s \approx (-v_F/t)k \lambda e^{-i\lambda\theta}$, where $\lambda = \text{sgn}(s) = 1(-1)$ for $s = K_+(K_-)$, v_F is graphene Fermi's velocity, θ is the azimuthal angle of \mathbf{k} . The Hamiltonian of graphene is then

$$H_g = \sum_{s\sigma\mathbf{k}} v_F k \begin{pmatrix} a_{s\mathbf{k}\sigma}^\dagger & b_{s\mathbf{k}\sigma}^\dagger \end{pmatrix} \begin{pmatrix} 0 & \lambda e^{-i\lambda\theta} \\ \lambda e^{i\lambda\theta} & 0 \end{pmatrix} \begin{pmatrix} a_{s\mathbf{k}\sigma} \\ b_{s\mathbf{k}\sigma} \end{pmatrix}. \quad (2)$$

H_g is diagonalized by introducing the ζ fields [25] as

$$\begin{aligned} a_{s\mathbf{k}\sigma} &= \frac{1}{\sqrt{2}}[\zeta_{+\sigma}^s(\mathbf{k}) + \zeta_{-\sigma}^s(\mathbf{k})], \quad b_{s\mathbf{k}\sigma} = \frac{\lambda}{\sqrt{2}}e^{i\lambda\theta}[\zeta_{+\sigma}^s(\mathbf{k}) - \zeta_{-\sigma}^s(\mathbf{k})], \\ H_g &= \sum_{s\sigma\mathbf{k}} \left[v_F |k| \zeta_{+\sigma}^{s\dagger}(\mathbf{k}) \zeta_{+\sigma}^s(\mathbf{k}) - v_F |k| \zeta_{-\sigma}^{s\dagger}(\mathbf{k}) \zeta_{-\sigma}^s(\mathbf{k}) \right]. \end{aligned} \quad (3)$$

Partial wave method and hybridization Hamiltonian

Going over from a discrete to a continuum \mathbf{k} [26] we write $H_g = \sum_{s\sigma} \int d\mathbf{k} \left[v_F |k| \zeta_{+\sigma}^{s\dagger}(\mathbf{k}) \zeta_{+\sigma}^s(\mathbf{k}) - v_F |k| \zeta_{-\sigma}^{s\dagger}(\mathbf{k}) \zeta_{-\sigma}^s(\mathbf{k}) \right]$, and $H_{\text{hyb}} = \frac{(N\Omega_0)^{1/2}}{2\pi} \sum_{s\sigma} \int d\mathbf{k} \left[\left(V_{s\mathbf{k}}^{Af} a_{s\mathbf{k}\sigma}^\dagger f_\sigma + V_{s\mathbf{k}}^{Bf} b_{s\mathbf{k}\sigma}^\dagger f_\sigma \right) + h.c. \right]$. Ω_0 is the unit cell area. In 2D orbital momentum eigenfunctions $e^{im\theta}$ we write $\zeta_{\pm\sigma}^s(\mathbf{k}) = \frac{1}{\sqrt{|k|}} \sum_{m=-\infty}^{\infty} \frac{1}{\sqrt{2\pi}} e^{im\theta} \zeta_{\pm\sigma}^{ms}(k)$, where $\{\zeta_{v\sigma}^{ms}(k), \zeta_{v'\sigma'}^{m's'\dagger}(k')\} = \delta_{ss'} \delta_{vv'} \delta_{\sigma\sigma'} \delta_{mm'} \delta(k - k')$. H_g is then expressed as

$$H_g = \sum_{ms\sigma} \int_0^\infty v_F |k| dk \left[\zeta_{+\sigma}^{ms\dagger}(k) \zeta_{+\sigma}^{ms}(k) - \zeta_{-\sigma}^{ms\dagger}(k) \zeta_{-\sigma}^{ms}(k) \right]. \quad (4)$$

For discussing the hybridization Hamiltonian for various geometric configurations we set the spatial zero point "O" as the projection of impurity position onto the unit cell.

Adatom impurity above one A atom (ADA): In this case $\tau_A = 0$, in the Dirac cones we find (we assume v_0 is real) $V_{s\mathbf{k}}^{Af} = \frac{V^{Af}(0)}{\sqrt{N}} = \frac{v_0}{\sqrt{N}}$. The next nearest neighbors are three B atoms at $\delta_i, i = 1, 2, 3$. Thus, $V_{s\mathbf{k}}^{Bf} = \frac{\Phi^*(\mathbf{k}) V^{Bf}}{\sqrt{N}} = \lambda \frac{v_F k v_1 e^{i\lambda\theta}}{-t\sqrt{N}}$, where $v_1 = V^{Bf}$. Substituting in H_{hyb} we find

$$H_{\text{hyb}} = \sum_{s\sigma} \int_0^\infty \frac{\sqrt{\pi\Omega_0|k|} dk}{2\pi} \left[v_0 (\zeta_{+\sigma}^{0,s\dagger}(k) + \zeta_{-\sigma}^{0,s\dagger}(k)) + \frac{v_1 v_F k}{-t} (\zeta_{+\sigma}^{0,s\dagger}(k) - \zeta_{-\sigma}^{0,s\dagger}(k)) \right] f_\sigma + h.c..$$

This equation tells us only $m = 0$ flavor couples to the impurity.

Adatom impurity above the center of the honeycomb: Here, the impurity hybridizes with the same strength v_0 , with 6 nearest neighbors, 3 A atoms and 3 B atoms. With respect to O, A_2, B_2, A_3, B_3 are in other unit cells. Three A(B) atoms yield $\Phi^*(\Phi)$ when the phases are coherently superimposed, i.e. $V_{\mathbf{k}}^{Af} a_{\mathbf{k}\sigma}^\dagger f_\sigma + V_{\mathbf{k}}^{Bf} b_{\mathbf{k}\sigma}^\dagger f_\sigma = \frac{v_0}{\sqrt{N}} \left[e^{-i\mathbf{k}\cdot\delta_3} (1 + e^{-i\mathbf{k}\cdot(\mathbf{a}_1+\mathbf{a}_2)} + e^{-i\mathbf{k}\cdot\mathbf{a}_1}) a_{\mathbf{k}\sigma}^\dagger f_\sigma + e^{i\mathbf{k}\cdot\delta_1} (1 + e^{-i\mathbf{k}\cdot\mathbf{a}_1} + e^{i\mathbf{k}\cdot\mathbf{a}_2}) b_{\mathbf{k}\sigma}^\dagger f_\sigma \right] = \frac{v_0}{\sqrt{N}} \left[\Phi^*(\mathbf{k}) a_{\mathbf{k}\sigma}^\dagger f_\sigma + \Phi(\mathbf{k}) b_{\mathbf{k}\sigma}^\dagger f_\sigma \right]$. For H_{hyb} we deduce

$$\begin{aligned} H_{\text{hyb}} &= \sqrt{\pi\Omega_0} \frac{v_0}{-t} \sum_{s\sigma} \lambda \int_0^\infty \frac{\sqrt{|k|} dk}{2\pi} v_F |k| \left(\left[(\zeta_{+\sigma}^{\lambda,s\dagger}(k) + \zeta_{-\sigma}^{\lambda,s\dagger}(k)) f_\sigma \right. \right. \\ &\quad \left. \left. + \lambda (\zeta_{+\sigma}^{-2\lambda,s\dagger}(k) - \zeta_{-\sigma}^{-2\lambda,s\dagger}(k)) f_\sigma \right] + h.c. \right). \end{aligned} \quad (5)$$

When $s = K_+$, $\lambda = 1$, the impurity couples with the partial wave $m = 1$ from A sublattice, and $m = -2$ from B sublattice. When $s = K_-$, $\lambda = -1$, it interacts with $m = -1$ from A sublattice, and $m = 2$ from B sublattice.

FLAVOR RIGHT MOVERS AND SYMMETRY ANALYSIS

We unfold the range of momenta k from $(0, \infty)$ to $(-\infty, +\infty)$ by defining flavor right movers. For ADA case applies $c_{1\sigma}^s(k) = \zeta_{+\sigma}^{0,s}(|k|)$, for $k > 0$ and $c_{1\sigma}^s(k) = \zeta_{-\sigma}^{0,s}(|k|)$, for $k < 0$. We obtain thus $H_g = \sum_{s\sigma} \int_{-\infty}^{\infty} \varepsilon_k dk c_{1\sigma}^{s\dagger}(k) c_{1\sigma}^s(k)$, $H_{\text{hyb}} = \sqrt{\pi\Omega_0} \sum_{s\sigma} \left[\int_{-\infty}^{\infty} \frac{\sqrt{|k|} dk}{2\pi} \left(v_0 + \frac{v_1 v_F k}{(-t)} \right) c_{1\sigma}^{s\dagger}(k) f_\sigma + h.c. \right]$, where $\varepsilon_k = \hbar v_F k$. So, the impurity couples with only one flavor of conducting waves. For ADC case the impurity couples with $m = \lambda$ or $m = -2\lambda$ flavors from A or B sublattices respectively. Therefore, we introduce two flavor right movers as $c_{1\sigma}^s = \lambda \zeta_{+\sigma}^{\lambda,s}(|k|)$, $c_{2\sigma}^s = \zeta_{+\sigma}^{-2\lambda,s}(|k|)$ for $k > 0$; $c_{1\sigma}^s = -\lambda \zeta_{-\sigma}^{\lambda,s}(|k|)$, $c_{2\sigma}^s = \zeta_{-\sigma}^{-2\lambda,s}(|k|)$ for $k < 0$. In terms of these, $H_g = \sum_{ns\sigma} \int_{-\infty}^{\infty} \varepsilon_k dk c_{n\sigma}^{s\dagger}(k) c_{n\sigma}^s(k)$, and $H_{\text{hyb}} = \frac{v_0 \sqrt{\pi\Omega_0}}{(-t)} \sum_{ns\sigma} \left[\int_{-\infty}^{\infty} \frac{\varepsilon_k \sqrt{|k|} dk}{2\pi} c_{n\sigma}^{s\dagger}(k) f_\sigma + h.c. \right]$, where $n = 1, 2$. In these two cases, we have $\{c_{n\sigma}^s(k), c_{n'\sigma'}^{s'\dagger}(k')\} = \delta_{nn'} \delta_{ss'} \delta_{\sigma\sigma'} \delta(k - k')$.

Symmetry analysis

The valence bands formed by σ bonds of sp^2 hybridization were discussed by Lomer long ago [27]. The popular tight-binding Hamiltonian for π and π^* bands formed by p_z orbitals located on each carbon atom was developed by Wallace [28], Slonczewski and Weiss [29]. A detailed single group analysis was given by Bassani and Parravicini [30]. Group theory has also been used [31] to analyze the Raman scattering and electron-phonon interaction. Trigonal band structure was analyzed in terms of graphene double group [32]. Here, we ignore z plane reflection and consider the C_{6v} point single group, and the little group at K_\pm as C_{3v} single group. The symmetry group elements for C_{3v} at Dirac points are E , C_3^+ , C_3^- , σ_{di} , where $i = 1, 2, 3$. The symmetry operation σ_{di} leaves the Dirac points unchanged but interchanges A by B atoms in real space. σ_{vi} acts the opposite way.

If we use $D^{\frac{1}{2}}$ to indicate the spinor reps for a rotation group, then for C_{3v} , $\Gamma_1 \otimes D^{\frac{1}{2}} = \Gamma_4$. We also have the relations $\Gamma_5 \otimes \Gamma_4 = \Gamma_3$, $\Gamma_6 \otimes \Gamma_4 = \Gamma_3$, and $\Gamma_4 \otimes \Gamma_4 = \Gamma_1 + \Gamma_2 + \Gamma_3$.

| C_{3v} | E | \bar{E} | C_3^+, C_3^- | \bar{C}_3^+, \bar{C}_3^- | σ_{di} | $\bar{\sigma}_{di}$ |
|------------|---|-----------|----------------|----------------------------|---------------|---------------------|
| Γ_1 | 1 | 1 | 1 | 1 | 1 | 1 |
| Γ_2 | 1 | 1 | 1 | 1 | -1 | -1 |
| Γ_3 | 2 | 2 | -1 | -1 | 0 | 0 |
| Γ_5 | 1 | -1 | -1 | 1 | i | -i |
| Γ_6 | 1 | -1 | -1 | 1 | -i | i |
| Γ_4 | 2 | -2 | 1 | -1 | 0 | 0 |

TABLE I: Character table for double group C_{3v} for K_{\pm} point of graphene. $\Gamma_{4,5,6}$ are extra representations (reps) and the spinor rep is Γ_4 .

Without spin and when the Fermi level E_F crosses K_{\pm} we have a Γ_3 reps. Following Ref. [29] we can show the Bloch sum for the p_z orbitals on A and B sublattices are the basis of the representation, i.e. $\phi_{\mathbf{k}}^{\alpha}(\mathbf{r}) = \frac{1}{\sqrt{N}} \sum_{\mathbf{R}_i} e^{-i\mathbf{k} \cdot (\mathbf{R}_i + \boldsymbol{\tau}_{\alpha})} \phi_i^{\alpha}(\mathbf{r} - \mathbf{R}_i - \boldsymbol{\tau}_{\alpha})$, where $\alpha = A$ or B , ϕ_i^{α} representing p_z orbital at $\mathbf{R}_i + \boldsymbol{\tau}_{\alpha}$ site. When spin is taken into account and spin orbit interaction (SOI) is ignored, the degeneracy at K_{\pm} is $2 \times 2 = 4$. When SOI is considered, the reps of double group are split into $\Gamma_3 \otimes D^{\frac{1}{2}} = \Gamma_4 + \Gamma_5 + \Gamma_6$. The reps Γ_4, Γ_5 , and Γ_6 are degenerate in absence of SOI at K_{\pm} .

a) For *ADA case* the system has a \bar{C}_{3v} symmetry (different from C_{3v} , the character table is shown by table 1). The planes reflection symmetry in \bar{C}_{3v} converts the point K_+ into K_- and vice versa. Thus, the symmetry \bar{C}_{3v} mixes the states from the two Dirac points. In fact, this group is a subgroup of C_{6v} and the symmetry reflection planes do show up in C_{6v} and map Dirac points onto each others. Thus, only one flavor couples with the impurity. The Hamiltonian in this case shows that a basis belonging to Γ_1 representation of \bar{C}_{3v} can be constructed from the E rep of C_{3v} , which leads to an invariant hybridization Hamiltonian.

If we consider explicitly a 3d magnetic impurity in this case, for example Mn (as realized in ADA case [33]), the nonvanishing coupling is only present between the d_{z^2} orbital of the impurity and graphene since the d_{z^2} orbital transforms according to Γ_1 rep.

b) For *ADC case* the symmetry group is C_{6v} where C_2 , $C_6^{+(-)}$ and σ_{vi} show up in this group except the symmetry operations in C_{3v} . In this group, C_2 , $C_6^{+(-)}$ transform A sublattice into B sublattice, K_+ into K_- and vice versa. σ_{vi} keep the sublattice unchanged but exchange K_+ and K_- . Therefore, we have to construct the basis for C_{6v} by using the basis for the two Dirac points in C_{3v} group. From Table 2, E rep in C_{3v} corresponds to the E_1 and E_2 reps in C_{6v} . Therefore we can use the Bloch sums $\phi_{K\pm\mathbf{k}\sigma}^{A(B)}$ in the E rep in C_{3v} to construct the reps in C_{6v} . Explicitly we consider a 3d magnetic element, and ignore the crystal electric field

| basis | | C_{6v} | C_{3v} |
|-------------------|----------------------|------------------|------------------|
| $x^2 + y^2, z^2$ | z | $A_1 (\Gamma_1)$ | $A_1 (\Gamma_1)$ |
| | R_z | $A_2 (\Gamma_2)$ | $A_2 (\Gamma_2)$ |
| (xz, yz) | $(x, y), (R_x, R_y)$ | $E_1 (\Gamma_5)$ | $E (\Gamma_3)$ |
| $(x^2 - y^2, xy)$ | | $E_2 (\Gamma_6)$ | |

TABLE II: Basis table of C_{6v} and C_{3v} and their compatibility relations. $R_x = yp_z - zp_y$ is the angular momentum component around axis x , the others are obtained by cyclic permutation.

splitting so that the energy levels for different reps are still degenerate or quasi-degenerate. The wave function should be constructed according to the symmetry group of C_{6v} . The reason is that the nonvanishing hybridization should be invariant under the operations in C_{6v} which is obtained as $\Gamma_i \otimes \Gamma_i$ by group theory. From Table 2, we infer d_{z^2} belongs to Γ_1 , (d_{xz}, d_{yz}) to $\Gamma_5(E_1)$, and $(d_{x^2-y^2}, d_{xy})$ to $\Gamma_6(E_2)$. These 3d orbitals are well defined. Having specified the states of the impurity, we consider the basis of C_{6v} reps by combining the basis

of E in C_{3v} . We find

$$\begin{aligned}\phi_{\mathbf{k}\sigma}^{\Gamma_5} &= (1/\sqrt{2})(\phi_{K+\mathbf{k}\sigma}^A - \omega\phi_{K-\mathbf{k}\sigma}^B, \phi_{K-\mathbf{k}\sigma}^A - \omega^*\phi_{K+\mathbf{k}\sigma}^B)^T, \\ \phi_{\mathbf{k}\sigma}^{\Gamma_6} &= (1/\sqrt{2})(\phi_{K+\mathbf{k}\sigma}^A + \omega\phi_{K-\mathbf{k}\sigma}^B, \phi_{K-\mathbf{k}\sigma}^A + \omega^*\phi_{K+\mathbf{k}\sigma}^B)^T,\end{aligned}\quad (6)$$

where $\omega = e^{i2\pi/3}$. Therefore, the hybridization Hamiltonian for 3d magnetic impurity is

$$H_{\text{hyb}} = \sum_{\alpha\mathbf{k}\sigma} \left(v_{\mathbf{k}}^{\alpha} c_{\alpha\mathbf{k}\sigma}^{\dagger} f_{\alpha\sigma} + h.c. \right), \quad (7)$$

where $\alpha = \Gamma_1, \Gamma_5, \Gamma_6$ reps, and the latter two are 2D reps. The creation and annihilation operators are obtained by defining the field operators based on the respective basis of the corresponding rep in the standard way. This situation resembles the Coqblin - Schrieffer model [34], however the Hamiltonian now is written in terms of the irreducible reps of the systems.

Kondo temperature under large U . - We calculated the Kondo temperature for the Anderson model in ADA case using the equation of motion method [35] that gives consistent results for the susceptibility with those derived by other methods at high temperature [36] and delivers the correct Kondo temperature [37]. The Kondo temperature for large U is proportional to $\exp \frac{\pi(\varepsilon_0 - \mu)}{\Delta|\mu|}$, where $\Delta = \frac{\pi v_0^2}{D^2}$, D is the energy cutoff. If $\varepsilon < \mu$ and $\mu \rightarrow 0$, the Kondo temperature tends to zero. The impurity is then decoupled from graphene. If $\varepsilon < \mu$ and with increasing $|\mu|$ the Kondo temperature increases exponentially. Thus, a small gate voltage may change the Kondo temperature dramatically [9].

CONCLUDING REMARKS

Summarizing, we investigated the Kondo model for a magnetic impurity in graphene in an adatom configuration. Starting from the tight-binding Anderson model we applied a partial wave method to expose the coupling flavors. The Kondo effect in graphene behaves as follows: *i)* For ADA case, only one flavor couples to the impurity. *ii)* For the ADC case, the number of channels is determined by the multiplets of the impurity as well. Multi-flavor character shows up in this case. *iii)* Based on the irreducible basis of the reps of the system, A Coqblin-Schrieffer-like hybridization model is derived for a 3d magnetic atom. d_{z^2} , (d_{xz}, d_{yz}) , and $(d_{x^2-y^2}, d_{xy})$ couple with the Γ_1 , $\Gamma_5(E_1)$, and $\Gamma_6(E_2)$ reps respectively. The bases for these reps of graphene are derived explicitly. *iiii)* The degeneracy of the

two Dirac points only leads to a higher T_K for ADA case. Applying a gate voltage the exchange coefficients are non-zero due to a finite DOS at E_F and the Kondo effect should be observable.

We thank C.-L. Jia, M.A.N. Araújo and A. Rosch for useful discussions. The work is supported by the excellence cluster "Nanostructured Materials" of the state Saxony-Anhalt.

-
- [1] K. S. Novoselov, *et al.*, Science **306**, 666 (2004); Y. Zhang, *et al.*, Phys. Rev. Lett. **94**, 176803 (2005); C. Berger, *et al.*, J. Phys. Chem. B **108**, 19912 (2004).
 - [2] A. H. Castro Neto, *et al.*, Rev. Mod. Phys. **81**, 109 (2009).
 - [3] J.C. Meyer *et al.*, Nature **454**, 319 (2008).
 - [4] B. Uchoa, *et al.*, Phys. Rev. Lett. **101**, 026805 (2008).
 - [5] K.-H. Ding, Z.-G. Zhu, J. Berakdar, J. Phys.: Condens. Matter **21**, 182002 (2009).
 - [6] B. Uchoa, *et al.*, arXiv.0906.2779.
 - [7] M. Hentschel and F. Guinea, Phys. Rev. B **76**, 115407 (2007).
 - [8] B. Dóra, and P. Thalmeier, Phys. Rev. B **76**, 115435 (2007).
 - [9] K. Sengupta and G. Baskaran, Phys. Rev. B **77**, 045417 (2008).
 - [10] P. S. Cornaglia, *et al.*, Phys. Rev. Lett. **102**, 046801 (2009).
 - [11] H.-B. Zhuang, *et al.*, arXiv: 0905.4548.
 - [12] P. Nozières and A. Blandin, J. Phys. (Paris) **41**, 193 (1980); P. Schlottmann and P. D. Sacramento, Adv. Phys. **42**, 641 (1993) and references therein.
 - [13] D. L. Cox and A. Zawadowski, Adv. Phys. **47**, 599 (1998).
 - [14] D. L. Cox, and M. Jarrell, J. Phys.: Condens. Matters **8**, 9825 (1996).
 - [15] C. M. Varma, *et al.*, Phys. Rep. **361**, 267 (2002).
 - [16] B. Uchoa, *et al.* Phys. Rev. Lett. **103**, 206804 (2009).
 - [17] K. Saha, I. Paul, and K. Sengupta, Phys. Rev. B **81**, 165446 (2010).
 - [18] T. O. Wehling, *et al.* Arxiv: 0906.2426v1.
 - [19] P. W. Anderson, Phys. Rev. **124**, 41 (1961).
 - [20] A. C. Hewson, *The Kondo problem to heavy fermions*, (Cambridge Uni. Press, 1993).
 - [21] G. W. Semenoff, Phys. Rev. Lett. **53**, 2449 (1984).
 - [22] V. P. Gusynin, *et al.*, Inter. J. Mod. Phys. B **21**, 4611 (2007).

- [23] D. P. DiVincenzo and E. J. Mele, Phys. Rev. B **29**, 1685 (1984).
- [24] J. C. Slater, and G. F. Koster, Phys. Rev. **94**, 1498 (1954).
- [25] C. R. Cassanello, and E. Fradkin, Phys. Rev. B **53**, 15079 (1996).
- [26] H. R. Krishna-Murthy, J. W. Wilkins, and K. G. Wilson, Phys. Rev. B **21**, 1003 (1980).
- [27] W. M. Lomer, Proc. Roy. Soc. London A **227**, 330 (1955).
- [28] P. R. Wallace, Phys. Rev. **71**, 622 (1947).
- [29] J. C. Slonczewski, and P. R. Weiss, Phys. Rev. **109**, 272 (1958).
- [30] F. Bassani, and G. P. Parravicini, Il Nuovo Cimento B **50**, 95 (1967).
- [31] D. M. Basko, I. L. Aleiner, Phys. Rev. B **77**, 041409 (2008).
- [32] R. Winkler, and U. Zülicke, arXiv: 0807.4204 (2009).
- [33] *D. M. Duffy, and J. A. Blackman, Phys. Rev. B* **58**, 7443 (1998).
- [34] J. R. Schrieffer, J. Appl. Phys. **38**, 1143 (1967); B. Coqblin, and J. R. Schrieffer, Phys. Rev. **185**, 847 (1969).
- [35] C. Lacroix, J. Phys. F: Metal Phys. **11**, 2389 (1981); J. Appl. Phys. **53**, 2131 (1982).
- [36] V. Kashcheyevs, *et al.*, Phys. Rev. B **73**, 125338 (2006).
- [37] H.-G. Luo, *et al.*, Phys. Rev. B **59**, 9710 (1999).